Inorganic Chemistry

pubs.acs.org/IC

Communication

Chemistry of Metal Silicates and Germanates: The Largest Metal Polygermanate, $K_{11}Mn_{21}Ge_{32}O_{86}(OH)_9(H_2O)$, with a 76 Å Periodic Lattice

Megan M. Smart, Colin D. McMillen, Kimberly Ivey, and Joseph W. Kolis*

Cite This: *Inorg. Chem.* 2020, 59, 16804−16808

Read Online

ACCESS | Metrics & More | Article Recommendations | Supporting Information

ABSTRACT: An examination of manganese silicates and germanates revealed unusual structural motifs and extremely different chemistries, with identical hydrothermal reactions forming $K_2Mn_2Si_3O_9$ versus $K_{11}Mn_{21}Ge_{32}O_{86}(OH)_9(H_2O)$. The germanate is exceptional in both its *c*-axis length (exceeding 76 Å) and unit cell volume (nearly 18000 Å^3), the largest known polygermanate structure to our knowledge.

Downloaded via CLEMSON UNIV on February 24, 2021 at 19:51:56 (UTC).
See https://pubs.acs.org/sharingguidelines for options on how to legitimately share published articles.

The oxyanions of silicon and germanium can differ significantly in their coordination chemistry with metal ions primarily because silicon largely forms tetrahedral or corner-shared polytetrahedral building blocks, while germanium more commonly adopts a wider range of geometries beyond tetrahedral, including five- and six-coordinate polyhedra such as trigonal bypyramids, square pyramids, and octahedra.[1,2] Perhaps a more interesting question is whether there can be significant differences between the two elements when they *do* adopt the same tetrahedral geometry. Indeed, both silicates and germanates are capable of forming a variety of complex polyanions.[3−8]

There are numerous examples of structurally analogous silicate and germanate compounds in the literature, including the well-known quartz (SiO_2 and GeO_2),[9,10] olivine ($NaLnXO_4$; Ln = lanthanide; X = Si, Ge),[11,12] sodalite [$Na_8(Al_6X_6O_{24})A_2$; X = Si, Ge; A = halide],[13] and apatite [$NaLn_9(XO_4)_6O_2$; Ln = lanthanide; X = Si, Ge][14,15] structure types. Despite these well-known instances of similarities between silicates and germanates, it should not be immediately assumed that they will adopt identical structures or physical properties. The modest size difference between four-coordinate silicon and germanium can potentially favor the formation of different structures for silicates and germanates given otherwise identical chemical reactions.

We employ hydrothermal synthesis as a route to metal oxyanions to explore interesting structure−property relationships and to probe the phase space, which is less well explored compared to more traditional flux synthesis.[16−18] In this way, the silicates and germanates provide an excellent test bed because SiO_2 and GeO_2 are both amphoteric oxides amenable to hydrothermal chemistry. We previously observed new chemistry with some complex and elegant structures resulting from the condensation of silicate tetrahedra into a variety of polysilicate chains and rings,[19,20] including the $Cs_3RESi_6O_{15}$ (RE = Dy−Lu, Y, In) structures featuring an elongated 57 Å *c* axis.[21] In general, germanates tend to be far less studied than silicates, although they also appear to have a very rich chemistry. Recent examinations of metal germanates in hydrothermal fluids have likewise shown great promise.[1,22−25]

Herein we present a case where the synthetic and structural chemistries of metal silicates and germanates differ dramatically from one another even though the oxyanions both adopt exclusively tetrahedral building blocks. In this study, identical synthetic reactions of 2:3 molar ratios of MnO and XO_2 (X = Si, Ge) produce $K_2Mn_2Si_3O_9$ (**1**) and $K_{11}Mn_{21}Ge_{32}O_{86}(OH)_9(H_2O)$ (**2**), respectively.[26] Both the resulting silicate and germanate have nearly ideal 2:3 ratios of Mn:Si/Ge (Figures S1 and S2), closely reflecting the starting ratios of the reactants. In both cases, the products were obtained in high yield [powder X-ray diffraction (PXRD); Figures S3 and S4], as very pale-pink and yellow rhombic crystals, respectively. The silicate and germanate have very different structures (Tables S1−S3), and the germanate was ultimately found to have a unit cell volume nearly 40 times that of the silicate.[27,28] A striking feature of **2** is a *c* axis that exceeds 76 Å in length (Figure S5). Both compounds are constructed from tetrahedral oxyanion building blocks, and both contain Mn^{2+} ions, so these two widely varying structures are not driven by the ability of germanium to adopt higher coordination numbers.

Although it is a much simpler structure than the germanate, the silicate **1** is not without interesting structural features. It crystallizes in the noncentrosymmetric, polar space group *Pn* and bears relation to $Rb_2Ca_2Si_3O_9$.[29] The structure is composed of two types of chains fused into a manganese silicate framework (Figure 1). The potassium atoms are found in the framework voids. Three unique silicon atoms form a metasilicate chain, $(SiO_3)_n$, via corner sharing, propagating

Received: August 3, 2020
Published: November 22, 2020

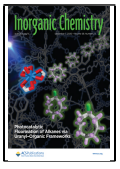

© 2020 American Chemical Society

https://dx.doi.org/10.1021/acs.inorgchem.0c02303
Inorg. Chem. 2020, 59, 16804−16808

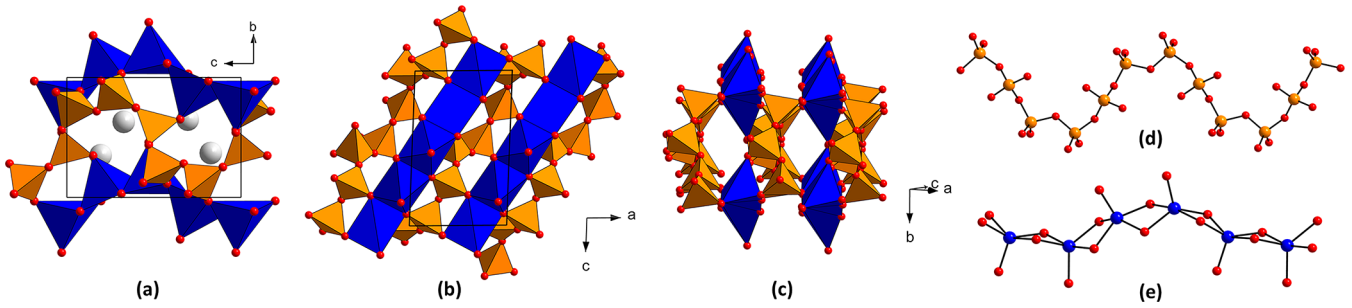

Figure 1. (a) Extended unit cell of **1**. Color scheme: silicon, orange polyhedra; manganese, blue polyhedra; oxygen, red spheres; potassium, silver spheres. (b) Connectivity of $(SiO_3)_n$ and $(MnO_3)_n$ chains into the manganese silicate framework. (c) Manganese silicate framework viewed along the direction of chain propagation. (d) Corner-sharing connectivity of silicate tetrahedra into $(SiO_3)_n$ chains. (e) Edge-sharing connectivity of square-pyramidal and trigonal-bipyramidal MnO_5 units into $(MnO_3)_n$ chains. Potassium atoms are omitted from parts b–e for clarity.

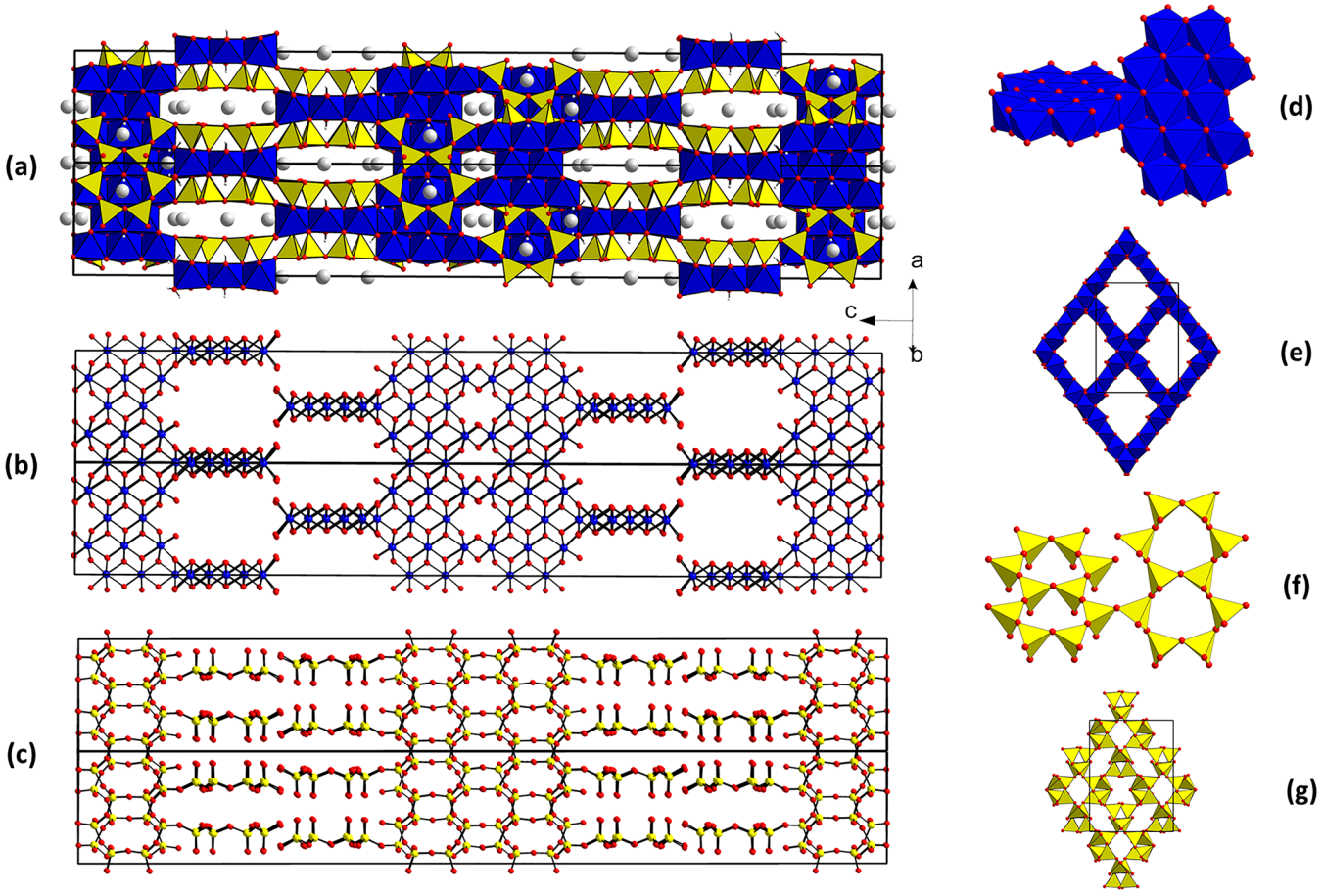

Figure 2. (a) Unit cell of **2**. (b) Manganese oxide sublattice of **2**. (c) Germanium oxide sublattice of **2**. (d) Connectivity and intersection of manganese oxide octahedra, forming the manganese oxide slab sublattice. (e) One layer of manganese oxide sublattice viewed along the *c* axis. (f) Connectivity and intersection of germanium oxide tetrahedra, forming the germanium oxide slab sublattice. (g) Two interpenetrating germanium oxide slabs corresponding to the manganese oxide slab in part e. Color scheme: germanium, yellow polyhedra and spheres; manganese, blue polyhedra and spheres; oxygen, red spheres; potassium, silver spheres.

along the *ac* face diagonal and imparting a polar sense to the structure. The bridging Si–O–Si angles are, on average, similar to those in pyroxenes, although they occur over a wider range [124.87(15)°–149.80(15)°] in **1** and with three unique kinking angles between bridging oxygen atoms, ranging from 112.75(16)° to 159.56(16)°.[30] This gives the silicate chains of **1** a wavelike appearance, with the nonbridging oxygen atoms on the silicate groups forming Si–O–Mn connections. The two unique manganese atoms are both five-coordinate with oxygen and form a one-dimensional substructure that also propagates along the *ac* face diagonal, flanking the silicate chains. The divalent five-coordinate manganese sites do not share the same geometry; Mn(1) is closer to an ideal square pyramid, while Mn(2) favors a distorted trigonal bipyramid, as shown by their respective τ_5 values of 0.01 and 0.57.[31] The manganese oxide chains, $(MnO_3)_n$, propagate by edge sharing, alternating between the square-pyramidal and trigonal-bipyramidal/prismatic sites, resulting in a shallow corrugation of the chains (Figure 1). To our knowledge, this arrangement of mixed MnO_5 coordination in a discrete Mn^{2+} chain has not

https://dx.doi.org/10.1021/acs.inorgchem.0c02303
Inorg. Chem. 2020, 59, 16804–16808

Table 1. Structural Parameters of Silicates and Germanates Having a Unit Cell Axis Greater than 65 Å as Reported in the Inorganic Crystal Structure Database

compound	a (Å)	b (Å)	c (Å)	V (Å^3)	space group	ref
$K_{11}Mn_{21}Ge_{32}O_{86}(OH)_9(H_2O)$	13.2676(8)	17.6436(11)	76.293(5)	17859.3	*Fddd*	this work
$(K_{12.64}Na_{30.23}Ca_{6.99})(Si_{36}Al_{36}O_{144})(SO_4)_{14.66}(H_2O)_{1.88}$	12.8770(7)	12.8770(7)	95.244(6)	13677.2	*R*32	33
$(Na_{79.84}Ca_{29.2}K_{14.78})(Al_{96}Si_{102}O_{396})(SO_4)_{31}Cl_2(H_2O)_6$	12.8742(6)	12.8742(6)	87.215(3)	12518.8	$P\bar{3}$	34
$(Mn_{19.50}Mg_{4.44})(V_{2.38}As_{1.12}Si_{2.76})O_{27.3}(OH)_{21.3}$	8.259(2)	8.259(2)	204.3(3)	12068.5	$R\bar{3}c$	35
$Na_{52}Ca_{36}K_{21}(SO_4)_{26}(Si_{90}Al_{90}O_{360})Cl_3(H_2O)_6$	12.913(1)	12.913(1)	79.605(5)	11495.4	*P*3	36
$Pb_{2.04}(Mn_{2.70}Zn_{0.30})(Fe_{1.76}Al_{0.04}Mn_{0.20})(Mn_{18.33}Mg_{0.23}Ca_{0.05})As_{2.16}(Si_{5.85}As_{0.21})O_{30}(OH)_{18.10}Cl_{5.90}$	8.257(2)	8.257(2)	126.59(4)	7474.4	$R\bar{3}c$	37
$Ba_{4.98}((Ca_{8.99}Sr_{0.96}Fe_{0.42}Na_{0.20})(Ce_{7.49}Th_{0.39}U_{0.17})Y_{3.53})(Ti_{11.86}Nb_{5.30})(SiO_4)_4((SiO_4)_{0.66}(PO_4)_{3.12})(BO_3)_9O_{21.88}((OH)_{41}F_2)(H_2O)_{1.5}$	9.1202(2)	9.1202(2)	102.145(5)	7357.9	*R*3	38
$Ba_2Ca_5Mn_2Fe_2(Pb_{18}Si_{30}O_{90})Cl(H_2O)_6$	9.865(2)	9.865(2)	79.45(1)	6696.0	$R\bar{3}$	39
$Mg_{45}Si_{32}O_{80}(OH)_{58}$	81.664(10)	9.255(5)	7.261(5)	5486.2	*C*2/*m*	40
Ca_3GeO_5	7.228(2)	7.228(2)	67.42(2)	3050.4	*R*3*m*	41

yet been reported in the literature, although square-pyramidal MnO_5 units connected into edge-sharing $(MnO_3)_n$ are reported for β-$LiMnBO_3$.[32]

The crystal structure of **2** is significantly more complex than that of the silicate analogue, with an exceptional 76 Å crystallographic *c* axis (Figure 2). The structure consists of interpenetrating slabs of edge-sharing MnO_6 octahedra and corner-sharing GeO_4 tetrahedra. The respective sublattices are fused by Mn−O−Ge corner sharing into a three-dimensional framework. Manganese oxide slabs are formed in the *ab* plane, and four slabs stack in an offset fashion to one another along the length of the *c* axis. Each large slab consists of individual slab substructures that intersect to form diamond-shaped openings (Figure 2). The Mn(6) atom serves as the hinge between X-shaped intersections of "subslabs". The GeO_4 tetrahedra form a complementary motif where six tetrahedra form rings via shared oxygen vertices. Rings are then fused into chains of rings, and these chains of rings are then cross-linked in an X-shaped fashion through O(15) vertices to also form slabs with similar diamond-shaped openings. Two such $(Ge_{16}O_{43})_n$ germanate sublattices interpenetrate the manganese oxide slabs and connect manganese oxide slabs along the *c* axis into a continuous manganese germanate framework. When viewed along the *ab* face diagonal, the channels in the manganese germanate framework are revealed, accommodating the potassium atoms of the structure.

The nearly colorless nature of the crystals (particularly for such a dense manganese oxide network), the Mn−O bond lengths [2.084(4)−2.342(4) Å], and the bond valence sums (BVSs) of the manganese sites are all consistent with six-coordinate Mn^{2+} (Tables S4 and S5). As such, hydrogen atoms assigned to the OH and H_2O groups are necessary for charge balance. Underbonded oxygen atoms were identified by their BVSs, and appropriate hydrogen atoms were assigned from the difference electron density map. In two of these OH groups, the hydrogen atom extends into the void at the center of the germanate rings fused to the manganese oxide slab, while the third is assigned as a mixed OH/H_2O site at the hinge of the slab. Their presence was verified by Fourier transform infrared spectroscopy (Figure S6), which exhibited absorption features at 3100, 3585, and 3650 cm^{-1}, all corresponding to O−H stretching modes, as well as an absorption feature at around 1600 cm^{-1} corresponding to H−O−H bending modes.

There are a number of inorganic silicates and germanates featuring unusually large unit cell axes reported in the literature (Table 1).[33−41] Of the silicates, those having axes greater than 65 Å are primarily mineralogical samples and generally have great compositional complexity.[5,42] The germanates are obviously far less ubiquitous than the silicates in the mineral kingdom, so one would expect a smaller sampling of such exceptional structures. Indeed, the only ICSD entry for a germanate having any unit cell axis exceeding even 50 Å in length is the synthetic Ca_3GeO_5, with its structure refined as a 24-layer polytype having disordered germanium sites. In this way, the 76 Å *c* axis and nearly 18000 Å^3 volume of **2** establish it as extraordinary among germanates. Even when compared with the silicate-containing mineralogical superstructures of turtmannite,[35] wiklundite,[36] and byzantievite,[38] where unit cell axes exceed 100 Å, the total unit cell volume of **2** stands apart (Table 1). The only other reports of germanates with such large unit cell volumes are polyoxometalates that contain some germanate components, although not as extended structural building blocks.[43−45] Thus, compound **2** in the present study is exceptional for polygermanates in terms of both its long axis length and its massive unit cell volume. Of course, many of these examples, including the title compound, are based on centered unit cells. Even so, the 38.719(5) Å *c* axis of the primitive reduced cell of **2** eclipses the 37.610(10) Å axis of $Nd_2Ge_2O_7$,[46] the next-longest primitive reduced cell axis reported for a germanate that is not part of a polyoxometallate species. Using the method of Krivovichev to quantify the level of complexity in the unit cell, we calculate that the IG value per unit cell is 1911 bits, which is in the "very complex" classification.[5,42] Comparatively, the silicate **1** only has a complexity of 128 bits per unit cell. The complexity values for the other compounds in Table 1 are given in Figure S7.

Despite the essentially identical synthesis conditions, the silicate and germanate synthons form two extremely different products in good yield, implying significantly different chemical behaviors in the two otherwise similar semimetal oxyanions. We postulate that these differences in the synthetic and crystal chemistry are driven by the modest size difference between the germanate and silicate tetrahedra. For the larger germanate building blocks, a $(GeO_3)_n$ chain analogous to the $(SiO_3)_n$ chain in **1** would likely position the oxygen atoms in incompatible positions to be shared by the $(MnO_3)_n$ chains built of the MnO_5 units without significantly distorting or destabilizing one of the constituent chains. The pyroxenes, $M^{2+}M^{2+}X^{4+}{}_2O_6$ (M = Ca, Mg, Mn, Fe, Co, Ni, Zn; X = Si, Ge), provide a useful example of how size matching between chains

https://dx.doi.org/10.1021/acs.inorgchem.0c02303
Inorg. Chem. 2020, 59, 16804−16808

of divalent transition-metal octahedra and the $(Si/GeO_3)_n$ chains can distort the chains to stabilize subtly different structures.[30,47−49] In this case, the structures of **1** and **2** represent a more dramatic extension of this concept, where very different structural building blocks stabilize the 2:3 combination of Mn:Si versus Mn:Ge. The presence of excess potassium hydroxide in both solutions allows K^+ to serve in a charge-balancing capacity to whatever degree is necessary for the different stable oxyanion frameworks. Subtle chemical factors may also play a role in distinguishing the silicate and germanate chemistries. For example, the more covalent nature of germanates compared to silicates, and the more basic nature of GeO_2 compared to SiO_2 may play a role in directing the in situ formation of different intermediate species that ultimately lead to different products.

For all of the complexity of **2**, its structure refines remarkably well, and all of the atom sites are well ordered. The fact that it forms as high-quality single crystals in good yield implies that the enormous unit cell is the stable packing arrangement of choice. We recently found a similar circumstance where hydrothermal synthesis led to a well-ordered superstructure of $Cs_3RESi_6O_{15}$ (RE = Dy−Lu, Y, In) having a *c*-axis length of 57 Å.[21] The 76 Å *c* axis and 17859 Å^3 unit cell volume of **2** stand in decidedly stark contrast to the silicate product **1** with its volume of only 451 Å^3. The presence of such curious new species emerging from these hydrothermal fluids implies that this synthetic medium is an excellent one for the formation of products of unusual complexity. It also confirms that the "simple" tetrahedral oxyanions are still robust and vibrant building blocks for new materials.

■ ASSOCIATED CONTENT

Supporting Information

The Supporting Information is available free of charge at https://pubs.acs.org/doi/10.1021/acs.inorgchem.0c02303.

Experimental and crystallographic details, bond lengths and angles, elemental analysis by energy-dispersive X-ray, PXRD patterns, IR spectra, and BVS calculations (PDF)

Accession Codes

CCDC 1997478 and 1997479 contain the supplementary crystallographic data for this paper. These data can be obtained free of charge via www.ccdc.cam.ac.uk/data_request/cif, or by emailing data_request@ccdc.cam.ac.uk, or by contacting The Cambridge Crystallographic Data Centre, 12 Union Road, Cambridge CB2 1EZ, UK; fax: +44 1223 336033.

■ AUTHOR INFORMATION

Corresponding Author

Joseph W. Kolis − *Department of Chemistry and Center for Optical Materials Science and Engineering Technologies, Clemson University, Clemson, South Carolina 29634, United States*; Email: kjoseph@clemson.edu

Authors

Megan M. Smart − *Department of Chemistry and Center for Optical Materials Science and Engineering Technologies, Clemson University, Clemson, South Carolina 29634, United States*

Colin D. McMillen − *Department of Chemistry and Center for Optical Materials Science and Engineering Technologies, Clemson University, Clemson, South Carolina 29634, United States*; orcid.org/0000-0002-7773-8797

Kimberly Ivey − *Department of Materials Science and Engineering, Clemson University, Clemson, South Carolina 29634, United States*

Complete contact information is available at: https://pubs.acs.org/10.1021/acs.inorgchem.0c02303

Notes

The authors declare no competing financial interest.

■ ACKNOWLEDGMENTS

We are indebted to the National Science Foundation (Grant DMR 1808371) for financial support of this work.

■ REFERENCES

(1) Nguyen, Q. B.; Lii, K.-H. $Cs_4UGe_8O_{20}$: A Tetravalent Uranium Germanate Containing Four- and Five-Coordinate Germanium. *Inorg. Chem.* **2011**, *50*, 9936−9938.

(2) Nguyen, Q. B.; Chen, C.-L.; Chiang, Y.-W.; Lii, K.-H. Cs3UGe7O18: A Pentavalent Uranium Germanate Containing Four- and Six-Coordinate Germanium. *Inorg. Chem.* **2012**, *51*, 3879−3882.

(3) Wierzbicka-Wieczorek, M.; Kolitsch, U. $BaYb_6(Si_2O_7)_2(Si_3O_{10})$ − the first silicate containing both Si_2O_7 and Si_3O_{10} groups: synthesis, crystal chemistry and topology. *Eur. J. Mineral.* **2013**, *25*, 509−517.

(4) Wierzbicka-Wieczorek, M.; Goeckeritz, M.; Kolitsch, U.; Lenz, C.; Giester, G. Two Structure Types Based on Si_6O_{15} Rings: Synthesis and Structural and Spectroscopic Characterisation of $Cs_{1.86}K_{1.14}DySi_6O_{15}$ and $Cs_{1.6}K_{1.4}SmSi_6O_{15}$. *Eur. J. Inorg. Chem.* **2015**, *2015*, 2426−2436.

(5) Krivovichev, S. V. Structural complexity of minerals: information storage and processing in the mineral world. *Mineral. Mag.* **2013**, *77*, 275−326.

(6) Dal Bo, F.; Aksenov, S. M.; Burns, P. C. A novel family of microporous uranyl germanates: Framework topology and complexity of the crystal structures. *J. Solid State Chem.* **2019**, *271*, 126−134.

(7) Juillerat, C. A.; Moore, E. E.; Morrison, G.; Smith, M. D.; Besmann, T.; zur Loye, H.-C. Versatile Uranyl Germanate Framework Hosting 12 Different Alkali Halide 1D Salt Inclusions. *Inorg. Chem.* **2018**, *57*, 11606−11615.

(8) Li, H.; Kegler, P.; Alekseev, E. V. Crystal growth of novel 3D skeleton uranyl germanium complexes: influence of synthetic conditions on crystal structures. *Dalton Trans* **2020**, *49*, 2244−2257.

(9) Bragg, W. L.; Gibbs, R. E. The structure of α and β quartz. *Proc. Royal Soc. A* **1925**, *109*, 405−427.

(10) Smith, G. S.; Isaacs, P. B. The crystal structure of quartz-like GeO_2. *Acta Crystallogr.* **1964**, *17*, 842−846.

(11) Yeon, J.; Hardaway, J. B.; Sefat, A. S.; Latshaw, A. M.; zur Loye, H.-C. Crystal growth, structures, magnetic and photoluminescent properties of $NaLnGeO_4$ (Ln = Sm, Eu, Gd, Tb). *Solid State Sci.* **2014**, *34*, 24−30.

(12) Emirdag-Eanes, M.; Krawiec, M.; Kolis, J. W. Hydrothermal synthesis and structural characterization of $NaLnGeO_4$ (Ln = Ho, Er, Tb, Tm, Yb, Lu) family of lanthanide germanates. *J. Chem. Crystallogr.* **2001**, *31*, 281−285.

(13) Fleet, M. E. Structures of sodium alumino-germanate sodalites $[Na_8(Al_6Ge_6O_{24})A_2$, A = Cl, Br, I]. *Acta Crystallogr., Sect. C: Cryst. Struct. Commun.* **1989**, *45*, 843−847.

(14) Ptacek, P. Rare-earth Element-bearing Apatites and Oxy-apatites. *Apatites and their Synthetic Analogues—Synthesis, Structure, Properties, and Applications*; IntechOpen, 2016; pp 245−288; DOI: 10.5772/62209.

(15) White, T. J.; ZhiLi, D. Structural derivation and crystal chemistry of apatites. *Acta Crystallogr., Sect. B: Struct. Sci.* **2003**, *B59*, 1−16.

(16) McMillen, C. D.; Kolis, J. W. Hydrothermal synthesis as a route to mineralogically-inspired structures. *Dalton Trans* **2016**, *45*, 2772−2784.
(17) Smith Pellizzeri, T. M.; McMillen, C. D.; Kolis, J. W. Alkali Transition-Metal Molybdates: A Stepwise Approach to Geometrically Frustrated Systems. *Chem. - Eur. J.* **2020**, *26*, 597−600.
(18) Smith Pellizzeri, T. M.; McMillen, C. D.; Wen, Y.; Chumanov, G.; Kolis, J. W. Three Unique Barium Manganese Vanadates from High-Temperature Hydrothermal Brines. *Inorg. Chem.* **2017**, *56*, 4206−4216.
(19) Mann, J. M.; McMillen, C. D.; Kolis, J. W. Crystal Chemistry of Alkali Thorium Silicates Under Hydrothermal Conditions. *Cryst. Growth Des.* **2015**, *15*, 2643−2651.
(20) Fulle, K.; Sanjeewa, L. D.; McMillen, C. D.; Kolis, J. W. Crystal chemistry and the role of ionic radius in rare earth tetrasilicates: $Ba_2RE_2Si_4O_{12}F_2$ (RE = Er^{3+}−Lu^{3+}) and $Ba_2RE_2Si_4O_{13}$ (RE = La^{3+}−Ho^{3+}). *Acta Crystallogr., Sect. B: Struct. Sci., Cryst. Eng. Mater.* **2017**, *73*, 907−915.
(21) Terry, R.; Vinton, D.; McMillen, C. D.; Kolis, J. W. A Cesium Rare-Earth Silicate $Cs_3RESi_6O_{15}$ (RE = Dy−Lu, Y, In): The Parent of an Unusual Structural Class Featuring a Remarkable 57 Å Unit Cell Axis. *Angew. Chem., Int. Ed.* **2018**, *57*, 2077−2080.
(22) Fulle, K.; Sanjeewa, L. D.; McMillen, C. D.; Wen, Y.; Rajamanthrilage, A. C.; Anker, J. N.; Chumanov, G.; Kolis, J. W. One-Pot Hydrothermal Synthesis of $Tb^{III}{}_{13}(GeO_4)_6O_7(OH)$ and $K_2Tb^{IV}Ge_2O_7$: Preparation of a Stable Terbium(4+) Complex. *Inorg. Chem.* **2017**, *56*, 6044−6047.
(23) Sanjeewa, L. D.; McGuire, M. A.; McMillen, C. D.; Garlea, V. O.; Kolis, J. W. Polar Materials with Isolated V^{4+} S = 1/2 Triangles: $NaSr_2V_3O_3(Ge_4O_{13})Cl$ and $KSr_2V_3O_3(Ge_4O_{13})Cl$. *Chem. Mater.* **2017**, *29*, 1404−1412.
(24) Li, H.; Kegler, P.; Bosbach, D.; Alekseev, E. V. Hydrothermal Synthesis, Study, and Classification of Microporous Uranium Silicates and Germanates. *Inorg. Chem.* **2018**, *57*, 4745−4756.
(25) Ferdov, S.; Lin, Z. The first hafnium germanate with garnet-type of structure: Mild hydrothermal synthesis, crystal structure and new mechanism of hydroxyl inclusion. *J. Solid State Chem.* **2019**, *273*, 117−121.
(26) Synthesis is achieved using MnO (0.074 g, 1.04 mmol) with SiO_2 (0.096 g, 1.6 mmol) or GeO_2 (0.17 g, 1.6 mmol) in aqueous 3−6 M KOH at 580 °C and 2 kbar; additional details are given in the Supporting Information.
(27) Crystallographic data of **1**: space group *Pn*, a = 6.3894(2) Å, b = 6.9661(2) Å, c = 10.1424(4) Å, β = 92.589(2)°, V = 450.97(3) Å^3, Z = 2, D = 3.066, 8187 reflections (2568 unique), R_1 = 0.0227, wR_2 = 0.0462.
(28) Crystallographic data of **2**: space group *Fddd*, a = 13.2676(8) Å, b = 17.6436(11) Å, c = 76.293(5) Å, V = 17859.3(19) Å^3, Z = 8, D = 4.057, 63287 reflections (4400 unique), R_1 = 0.0352, wR_2 = 0.0855.
(29) Kahlenberg, V.; Muellner, M.; Schmidmair, D.; Perfler, L.; Toebbens, D. M. $Rb_2Ca_2Si_3O_9$: the first rubidium calcium silicate. *Z. Kristallogr. Cryst. Mater.* **2016**, *231*, 209−217.
(30) Cameron, M.; Papike, J. J. Structural and chemical variations in pyroxenes. *Am. Mineral.* **1981**, *66*, 1−50.
(31) Addison, A. W.; Rao, T. N.; Reedijk, J.; van Rijn, J.; Verschoor, G. C. Synthesis, structure, and spectroscopic properties of copper(II) compounds containing nitrogen−sulphur donor ligands; the crystal and molecular structure of aqua[1,7-bis(N-methylbenzimidazol-2′-yl)-2,6-dithiaheptane]copper(II) perchlorate. *J. Chem. Soc., Dalton Trans.* **1984**, 1349−1356.
(32) Li, R. K.; Chen, C. T.; Greaves, C. Magnetic order of $LiMnBO_3$: A new type of chiral magnetic ground state. *Phys. Rev. B: Condens. Matter Mater. Phys.* **2002**, *66*, 052405.
(33) Camara, F.; Bellatreccia, F.; della Ventura, G.; Gunter, M. E.; Sebastiani, M.; Cavallo, A. Kircherite, a new mineral of the cancrinite-sodalite group with a 36-layer stacking sequence: Occurrence and crystal structure. *Am. Mineral.* **2012**, *97*, 1494−1504.
(34) Camara, F.; Bellatreccia, F.; della Ventura, G.; Mottana, A.; Bindi, L.; Gunter, M. E.; Sebastiani, M. Fantappièite, a new mineral of the cancrinite-sodalite group with a 33-layer stacking sequence: Occurrence and crystal structure. *Am. Mineral.* **2010**, *95*, 472−480.
(35) Brugger, J.; Armbruster, T.; Meisser, N.; Hejny, C.; Grobety, B. Description and crystal structure of turtmannite, a new mineral with a 68 Å period related to mcgovernite. *Am. Mineral.* **2001**, *86*, 1494−1505.
(36) Rastsvetaeva, R. K.; Chukanov, N. V. Model of the crystal structure of biachellaite as a new 30-layer member of the cancrinite group. *Crystallogr. Rep.* **2008**, *53*, 981−988.
(37) Cooper, M. A.; Hawthorne, F. C.; Langhof, J.; Halenius, U.; Holtstam, D. Wiklundite, ideally $Pb_2^{[4]}(Mn^{2+},Zn)_3(Fe^{3+},Mn^{2+})_2(Mn^{2+},Mg)_{19}(As^{3+}O_3)_2[(Si,As^{5+})O_4]_6(OH)_{18}Cl_6$, a new mineral from Långban, Filipstad, Värmland, Sweden: Description and crystal structure. *Mineral. Mag.* **2017**, *81*, 841−855.
(38) Sokolova, E.; Hawthorne, F. C.; Pautov, L. A.; Agakhanov, A. A. Byzantievite, $Ba_5(Ca,REE,Y)_{22}(Ti,Nb)_{18}(SiO_4)_4[(PO_4),(SiO_4)]_4(BO_3)_9O_{21}[(OH),F]_{43}(H_2O)_{1.5}$: the crystal structure and crystal chemistry of the only known mineral with the oxyanions (BO_3), (SiO_4) and (PO_4). *Mineral. Mag.* **2010**, *74*, 285−308.
(39) Grew, E. S.; Peacor, D. R.; Rouse, R. C.; Yates, M. G.; Su, S.-C.; Marquez, N. Hyttsjoite, a new complex layered plumbosilicate with unique tetrahedral sheets from Langban, Sweden. *Am. Mineral.* **1996**, *81*, 743−753.
(40) Capitani, G. C.; Mellini, M. The crystal structure of a second antigorite polysome (m = 16), by single-crystal synchrotron diffraction. *Am. Mineral.* **2006**, *91*, 394−399.
(41) Nishi, F.; Takeuchi, Y. 24-Layer structure of tricalcium germanate, Ca_3GeO_5. *Acta Crystallogr., Sect. B: Struct. Sci.* **1985**, *41*, 390−395.
(42) Krivovichev, S. V. Structure description, interpretation and classification in mineralogical crystallography. *Crystallogr. Rev.* **2017**, *23*, 2−71.
(43) Li, Z.; Lin, L.-D.; Yu, H.; Li, X.-X.; Zheng, S.-T. All-Inorganic Ionic Porous Material Based on Giant Spherical Polyoxometalates Containing Core-Shell K_6@K_{36}-Water Cage. *Angew. Chem., Int. Ed.* **2018**, *57*, 15777−15781.
(44) Ibrahim, M.; Mereacre, V.; Leblanc, N.; Wernsdorfer, W.; Anson, C. E.; Powell, A. K. Self-Assembly of a Giant Tetrahedral 3 d−4 f Single-Molecule Magnet within a Polyoxometalate System. *Angew. Chem., Int. Ed.* **2015**, *54*, 15574−15578.
(45) Li, S.; Liu, S. X.; Li, C.; Ma, F. J.; Liang, D.; Zhang, W.; Tan, R. K.; Zhang, Y.; Xu, L. Reactivity of Polyoxoniobates in Acidic Solution: Controllable Assembly and Disassembly Based on Niobium-Substituted Germanotungstates. *Chem. - Eur. J.* **2010**, *16*, 13435−13442.
(46) Vetter, G.; Queyroux, F.; Labbe, P. H.; Goreaud, M. Determination structurale de $Nd_2Ge_2O_7$. *J. Solid State Chem.* **1982**, *45*, 293−302.
(47) Redhammer, G. J.; Tippelt, G.; Reyer, A.; Gratzl, R.; Hiederer, A. Structural and Raman spectroscopic characterization of pyroxene-type compounds in the $CaCu_{1-x}Zn_xGe_2O_6$ solid-solution series. *Acta Crystallogr., Sect. B: Struct. Sci., Cryst. Eng. Mater.* **2017**, *73*, 419−431.
(48) Lambruschi, E. Effects of cation substitutions on the physical properties of $M_2M_1T_2O_6$ pyroxenes. Ph.D. Thesis, Universita Degli Studi di Parma, Parma, Italy, 2016.
(49) Redhammer, G. J.; Roth, G. A comparison of the clinopyroxene compounds $CaZnSi_2O_6$ and $CaZnGe_2O_6$. *Acta Crystallogr., Sect. C: Cryst. Struct. Commun.* **2005**, *61*, i20−i22.

https://dx.doi.org/10.1021/acs.inorgchem.0c02303
Inorg. Chem. 2020, 59, 16804−16808